# Blood Pressure Estimation Using Photoplethysmogram Signal and Its Morphological Features

Navid Hasanzadeh, Mohammad Mahdi Ahmadi, *Senior Member, IEEE,* and Hoda Mohammadzade

***Abstract*—In this paper, we present a machine learning model to estimate the blood pressure (BP) of a person using only his photoplethysmogram (PPG) signal. We propose algorithms to better detect some critical points of the PPG signal, such as systolic and diastolic peaks, dicrotic notch and inflection point. These algorithms are applicable to different PPG signal morphologies and improve the precision of feature extraction. We show that the logarithm of dicrotic notch reflection index, the ratio of low- to high-frequency components of heart rate (HR) variability signal, and the product of HR multiplied by the modified Normalized Pulse Volume (mNPV) are the key features in accurately estimating the BP using PPG signal. Our proposed method has achieved higher accuracies in estimating BP compared to the previously reported methods that only use PPG signal. For the systolic BP, the achieved correlation coefficient between the estimated values and the real values is 0.78, the mean absolute error of the estimated values is 8.22 mmHg, and their standard deviation is 10.38 mmHg. For the diastolic BP, the achieved correlation coefficient between the estimated and the real values is 0.72, the mean absolute error of the estimated values is 4.17 mmHg, and their standard deviation is 4.22 mmHg. The achieved results fall within Grade A for diastolic, Grade C for systolic and Grade B for mean BP based on BHS standard.**

***Index Terms*—Blood Pressure, Photoplethysmogram (PPG), Morphological Features, modified Normalized Pulse Volume, Machine Learning**

## I. Introduction

PLETHYSMOGRAM is a waveform representing the arterial oxygenation versus time. It is also a representation of blood volume versus time. If an optical method is used for sensing the plethysmogram signal, the obtained signal is called Photoplethysmogram (PPG). To record PPG, a red or infrared light is radiated to a body organ, such as fingertip or earlobe, and the reflected light is recorded. The amount of the reflected light is a measure of the arterial oxygen level [1]. Fig. 1 shows two pulses of a typical PPG signal.

PPG signal, by itself, is not directly related to blood pressure (BP), which is a measure of the pressure imposed by blood flow on the wall of vessels; however, subtle variation in the morphology of the PPG signal appears to be correlated to BP. To the best of our knowledge, presently there is no mathematical model backing this correlation and the relation between PPG and BP is currently only modelled with machine learning.

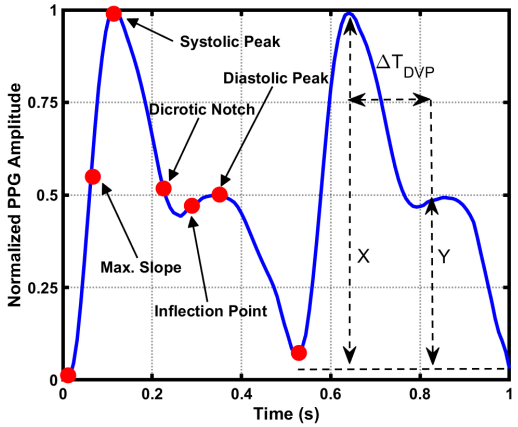


Fig. 1. Two pulse samples of a PPG signal. In the above figure, X and Y are the systolic peak and inflection points amplitudes respectively and $\Delta T_{DVP}$ is the time interval between the two.

If a method exists that can provide a reasonably accurate estimation of the BP of a person from his PPG, it provides several important advantages, including:

(1) It makes it possible to measure BP without using a cuff. This feature is very useful for people who find BP measurement using a cuff painful and annoying.

(2) It makes it possible to continuously measure the BP of a person. This feature is a significant advantage to cuff-based BP measurement approaches, because it makes possible to assess the BP of a person in different conditions, such as sleep, rest and other daily activities more realistically and accurately [2]. In addition, it has been shown that continuous monitoring of BP can help to significantly minimize the complications of high BP [3]–[5]. It also makes it possible to more thoroughly evaluate the effect of an antihypertensive agent [6].

(3) It makes it possible to use ordinary smartphones as simple sphygmomanometer as the built-in LED flash light of the cellphone can be used as a light source and the built-in CMOS camera as a photodetector, respectively. Fig. 2 shows a PPG signal recorded using iPhysioMeter App [7] running on an iPhone.

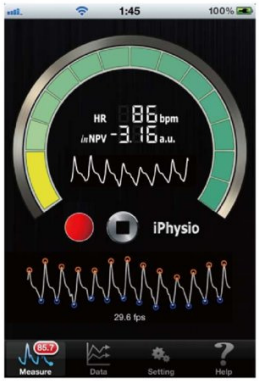


Fig. 2. A screenshot of iPhysiometer App [7] running on a smartphone, sensing PPG signal using LED light and camera of the phone.

Recently, a few methods have been presented to estimate BP using PPG signal [8]–[12]. The most common methods are based on measuring the propagation speed of blood from the heart to the body [13]. These methods, which are called, Pulse-Wave Velocity (PWV) based approaches, are based on the fact that PWV generally increases as the BP increases. An issue with the recently proposed PWV-based approaches is that they require measuring multiple electrophysiological signals. For example, the methods proposed in [14] require a combination of a PPG signal and an electrocardiogram (ECG), the method proposed in [15] requires PPG and a phonocardiogram (PCG), and the one proposed in [16] requires two PPG signals. As a result, the devices implemented based on these approaches are complex and cumbersome.

Matsumura *et al.* [17] proposed a method that requires only a PPG signal to estimate BP. The proposed method only uses heart rate and a feature called modified Normalized Pulse Volume (mNPV), proposed in [18], to estimate BP. mNPV is defined as the ratio of the peak-to-peak amplitude of a PPG signal divided by its dc value. Their proposed method achieved a good correlation between the estimated BP and its actual value, however, the size of their used dataset was too small to make reliable judgment about the accuracy of that method.

In this paper, we present a BP measurement algorithm which only uses the morphological features of a PPG signal. We extract Heart Rate Variability (HRV) signal from PPG and utilize some of its properties that have proven relations with autonomic nervous and cardiovascular systems. In addition, we use the mNPV feature to improve the accuracy of BP estimation. PPG pulses have different shapes in different individuals; as a result, the algorithms that are used for extracting features and detecting key points should have minimal sensitivities to these differences. We propose algorithms for robust detection of PPG key points such as minimum, systolic peak, diastolic peak and maximum slope point. Using these algorithms, we can more precisely detect the key points and thereby better extract physiological related features. As a result of these improvements, we have achieved more accurate BP estimation compared to the previously published methods using only PPG signal.

We also show that the logarithm of dicrotic notch reflection index (RI), the HRV low-frequency to high-frequency components ratio, and the product of Heart Rate (HR) multiplied by the modified Normalized Pulse Volume (mNPV) are the key features in estimating the BP using PPG signal. We have achived a correlation coefficient of 0.78 between the estimated and the real values of the systolic BP; the mean absolute error (MAE) of the estimated values is 8.22 mmHg, and their standard deviation (STD) is 10.38 mmHg. For the diastolic BP, we have achived a correlation coefficient of 0.72 between the estimated and the real values; the MAE of the estimated values is 4.17 mmHg, and their STD is 4.22 mmHg. The achieved results fall within Grade A for diastolic, Grade C for systolic and Grade B for mean BP based on BHS standard.

## II. Background

In this section, we briefly review the PPG signal and its key features used for BP estimation in this paper.

### A. Photoplethysmogram

As shown in Fig. 1, a PPG pulse has a few key points, such as maximum slope point, dicrotic notch, inflection point, and diastolic peak. Some PPG signals might be missing few of these points, such as diastolic peak.

The systolic peak happens when the blood pressure propagates from the left ventricle toward the fingertips. The diastolic peak is the result of the reflected blood pressure from small blood vessels in the lower part of the body towards the aorta and the fingertips [19].

### B. PPG Morphological Features

Due to differences in the cardiovascular systems, the shapes and morphologies of PPG signals vary from one person to another. Some extractable features from a PPG pulse are as follows:

#### 1) Heart Rate

Heart rate can be obtained by calculating the time interval between two consecutive systolic peaks or two consecutive minimums:

$$HR = \frac{60}{Peaks\ Interval\ (s)} \tag{1}$$

#### 2) Pulse Width

Awad *et al.* [20] define pulse width of a PPG signal as the time interval between the points at half height of the pulse and believe that it is correlated with the Systemic Vascular Resistance (SVR). SVR is the resistance against blood flow in the total vascular system except for pulmonary vessels and is calculated using [21]:

$$SVR = \frac{MAP - CVP}{CO} \tag{2}$$

where $CO$ represents cardiac output in terms of mL/min, $MAP$ is mean arterial BP in terms of mmHg and $CVP$ is the central venous pressure which is almost zero mmHg and can be

This article has been accepted for publication in a future issue of this journal, but has not been fully edited. Content may change prior to final publication. Citation information: DOI 10.1109/JSEN.2019.2961411, IEEE Sensors Journal



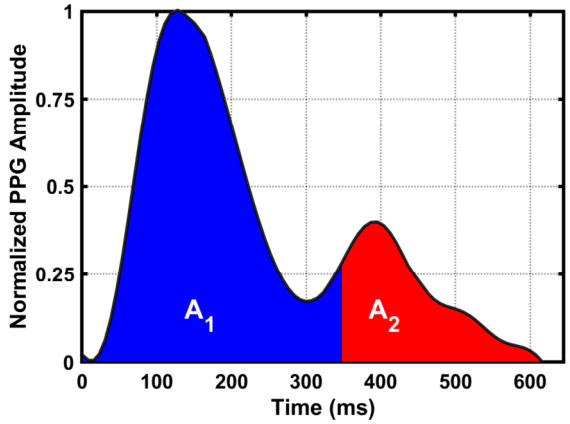


Fig. 3. The ratio of areas confined under PPG pulse is related to the total peripheral resistance and blood pressure.

neglected.

*3) Reflection Index*

Reflection index is a measure of pulse reflection in arteries and is related to the arterial tone which is the magnitude of blood vessel contraction in proportion to their maximum distensibility. RI is obtained using:

$$RI = \frac{Y}{X} \tag{3}$$

where $Y$ is the amplitude of the inflection point and $X$ is the amplitude of the systolic pulse [22].

*4) Large Artery Stiffness Index*

Large artery stiffness index of an individual is a measure of the stiffness of his arteries and is expressed by:

$$LASI = \frac{h}{\Delta T_{DVP}} \tag{4}$$

where $h$ is the height of the individual and $\Delta T_{DVP}$ is the time interval between the systolic peak and the inflection point of a PPG pulse [19]. Since the height of the subjects is not reported in our dataset, we set $h = 1$ for all subjects.

*5) Ratio of PPG Pulse Areas*

The ratio of PPG pulse areas is the ratio of different areas under a PPG pulse. By breaking the area under a PPG pulse into two parts based on the location of the inflection point, Wang *et al.* [23] showed that the ratio of these two areas is related to the total peripheral resistance and BP. Inflection Point Area ($IPA$) ratio is calculated from:

$$IPA = \frac{A_2}{A_1} \tag{5}$$

where $A_1$ and $A_2$ are the areas of the first and second parts as shown in Fig. 3.

*6) Crest Time*

Crest time is the time that it takes for the PPG signal to rise from its minimum point to its systolic peak. It has been shown that this index is related to PWV [24].

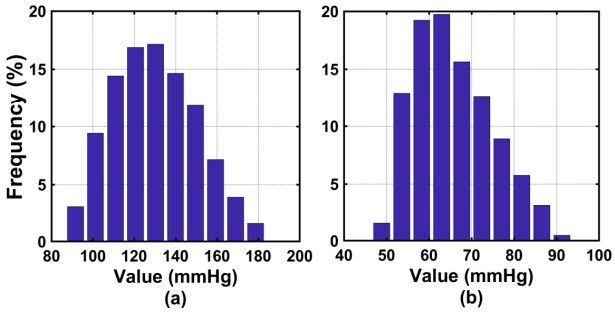


Fig. 4. Blood Pressure histograms of the used dataset. a) Systolic blood pressure. b) Diastolic blood pressure.

*7) Modified Normalized Pulse Volume (mNPV)*

This feature is expressed by:

$$mNPV = \frac{I_{ac}}{I_{ac} + I_{dc}} \tag{7}$$

where $I_{ac}$ is the peak-to-peak amplitude of the PPG pulse and $I_{dc}$ is the average of the pulse [17][18].

This feature is directly related to the pulsatile component of the arterial blood volume and is also related to total peripheral resistance (TPR) [25]–[27] which is linked to mean arterial pressure (MAP) by the following expression [19]:

$$MAP = CO * TPR \tag{6}$$

where $CO$ is cardiac output and is associated with heart rate[28][29]. Matsumura *et al.*[7] showed that mNPV is related to BP with a high correlation.

*8) Heart Rate Variability*

The HRV signal is a noninvasive marker of the performance of autonomic nervous and cardiovascular systems. It has been shown that the BP is correlated with the time-domain and frequency-domain properties of HRV [30][31][32]. HRV can be used to estimate the stress level of a person [33]. Although it is usually obtained by measuring the period of ECG signal, it can also be obtained by measuring the period of the PPG signal [34][35].

## C. Dataset

For the training and testing our proposed method, we have used cuff-less BP dataset available in Machine Learning repository of the University of California, Irvine (UCI) [14]. This dataset, which we call it *UCI dataset* in this paper, consists of 12000 signal parts of recorded ECG, PPG and Arterial Blood Pressure (ABP) from about 1000 individuals.

The source of this dataset was the Physionet's Multi-Parameter Intelligent Monitoring in Intensive Care Units (MIMIC II) [36], on which Kachuee *et al.* [14] have performed some pre-processing and validation. We have used the PPG signals as the input and the ABP signals as the target values. In Fig. 4, the histograms of the dataset for systolic and diastolic BPs are shown. The sampling rate of the recorded signals is 125Hz, which is sufficiently high to accurately extract the frequency-domain features of HRV[37]–[39].

# III. Proposed Method

Some of the features mentioned in Sec. II cannot be easily detected in a PPG signal, especially in those with abnormal BPs. In this paper, we present algorithms to effectively extract

This article has been accepted for publication in a future issue of this journal, but has not been fully edited. Content may change prior to final publication. Citation information: DOI 10.1109/JSEN.2019.2961411, IEEE Sensors Journal



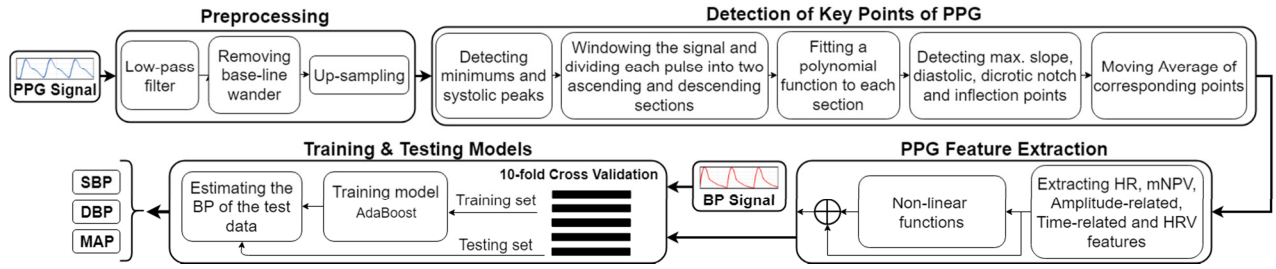


Fig 5. The block diagram of the proposed BP estimation algorithm.

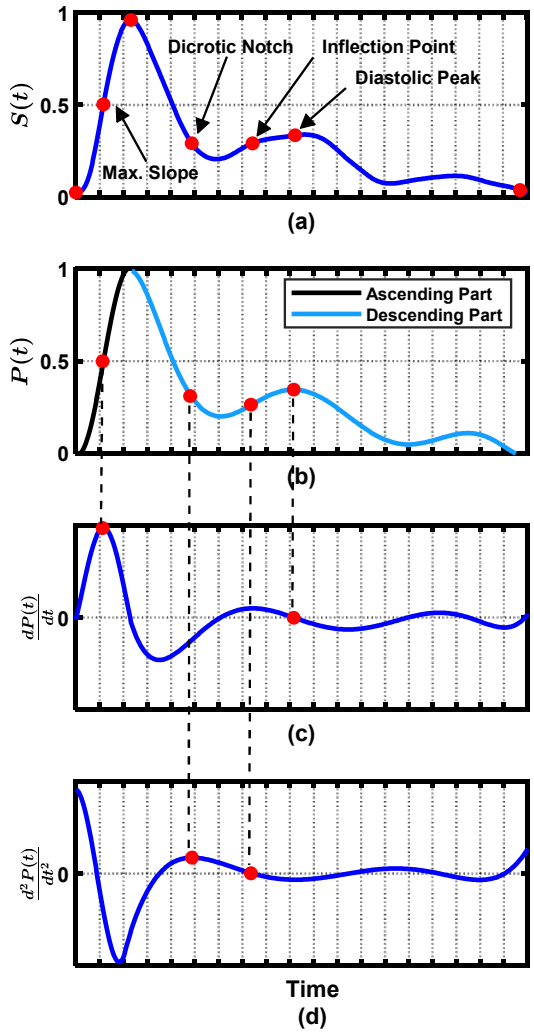


Fig. 6. The proposed technique and its implementation to detect the key points of a PPG pulse. a) The location of the key points. b) Dividing the pulse into two ascending and descending parts and fitting the polynomials that are shown in two different colors. c) The waveform of the first derivative of the polynomials which allows the detection of maximum slope point and the diastolic peak. d) The waveform of the second derivative of polynomials which allows the detection of the dicrotic notch and the inflection point.

the key features of a PPG signal. We also use more features compared to the ones used in previous works. Our proposed method consists of the following steps: 1) applying pre-processing algorithms on PPG signals for de-noising and removing base-line wandering, 2) detecting the key points of the PPG signals, 3) extracting the important features of the PPG signal, and 4) training the proposed BP estimation model using the available dataset. The block diagram of the proposed BP estimation algorithm is illustrated in Fig. 5.

### *A. Pre-processing*

In this step, a Type I Chebyshev low-pass filter with a cut-off frequency of 10 Hz is applied to the PPG signals. The filter was implemented using the forward-backward method to keep the group delay constant. The dc component of each signal is found using a moving median window and is subtracted from the filtered signal to make the signal dc-free. The dc-free signal which is free of any base-line wander, is used for extracting all features other than mNPV. For extracting the mNPV feature, the dc value of the signal is required.

After filtering, the signals are up-sampled from 125 Hz to 500 Hz in order to increase the detection accuracy of the key points.

### *B. Detection of Key Points*

Before extracting the features of the PPG signals, the key points of each pulse should be detected. These points are shown in Fig. 1 and also in Fig. 6(a). As PPG signals have different morphologies, the point detection algorithms should have minimal sensitivities to different morphologies. Here, we describe our proposed methods for detecting the key points:

#### *1) Detection of the Minimum Point and the Systolic Peak*

To detect the maximum and minimum points, different methods, such as window-thresholding techniques [40], combined Hilbert and wavelet transformation [41], artificial neural networks [42] and Kalman filtering [43], exist. A major issue with most of these methods is that their performance is highly dependent to the parameters such as the threshold value and the window length. To overcome this issue, we use Automatic Multiscale-based Peak Detection (AMPD) [44] method, which is useful for detecting the peaks of periodic and quasi-periodic signals.

In AMPD algorithm, the window size is automatically chosen, instead of specifying it in advance. In this method, the window size is swept from its minimum possible value to its maximum one, and the size of the window that results in the maximum number of local maxima is selected as the final window size. Then, at each window, the local maximum point, which is the maximum of that entire window is selected as one of the peaks of the signal. The result of applying this method on a sample of a PPG signal is illustrated in Fig. 7, indicating that the short-term variation of the dc of the signal does not

This article has been accepted for publication in a future issue of this journal, but has not been fully edited. Content may change prior to final publication. Citation information: DOI 10.1109/JSEN.2019.2961411, IEEE Sensors Journal



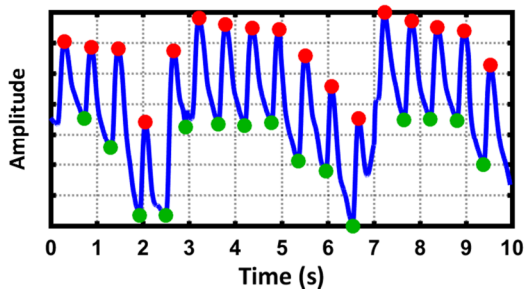


Fig. 7. A sample of implementation of Automatic Multiscale-based Peak Detection (AMPD) algorithm for detecting PPG signal systolic peaks and minimums.

affect the performance of the algorithm.

After detecting the minimum points and the systolic peaks, a single pulse lying between two consecutive minimums is selected and its amplitude is normalied to one. Then, the selected pulse is divided into two sections: one from the minimum point to the systolic peak, and the other from the systolic peak to the end. We call the first section as the *ascending section* and the second one as the *descending section* (See Fig. 6 (b)).

*2) Detection of Maximum Slope Point*

We use the first derivative of the PPG pulses to find the maximum slope point in the ascending section of the pulse. Usually, even after filtering, there are noise and unwanted artifacts on the PPG signals which are pronounced by taking the derivative of the signal. To avoid misdetection of the maximum slope point, we fit a $5^{th}$–order polynomial to the ascending section of the pulse. The maximum slope point is then detected by finding the point at which the fitted polynomial has the largest derivative (See Fig. 6 (b-c)).

*3) Detection of Diastolic Peak*

The diastolic peak is not easily noticeable in some PPG pulses [45]; consequently, we need to take the second derivative of the PPG signal in addition to the first one. Here, similar to the previous section, a polynomial is first fitted to the descending section of the waveform. To achieve a better fitting, the degree of the fitted polynomial to the descending section is chosen to be seven. We consider the diastolic peak to be the point at which the first derivative of the polynomial is equal to zero and the second derivative is negative. If there is no such point, then the point at which the second derivative is a local minimum is chosen as the diastolic peak.

*4) Detection of Dicrotic Notch*

The dicrotic notch is a point where the second derivative of the PPG signal is a local maximum and is located before the diastolic peak.

*5) Detection of Inflection Point*

The inflection point lies between the dicrotic notch and the diastolic peak. At this point, the second derivative of the PPG signal is equal to zero. If no such point exists, the inflection point is chosen to be the midpoint between the dicrotic notch and the diastolic peak.

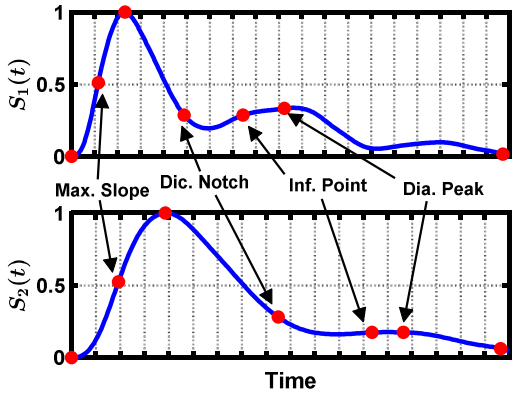


Fig. 8. Key point detection in two PPG signals with different morphologies.

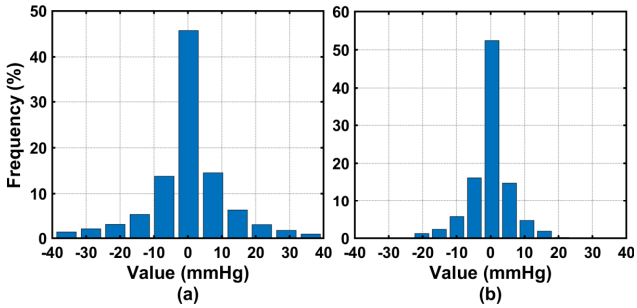


Fig. 9. Histograms of errors in AdaBoost model: a) systolic blood pressure, b) diastolic blood pressure.

After detecting the temporal locations of the key points, for each key point, we apply a moving average with the length of five pulses to remove the possible errors in the detection of the points. The length of the moving average window is considered as a hyperparameter and is tuned using the training set. Fig. 8 shows the result of applying the above point detection algorithms for two PPG pulses with different morphologies.

## C. Feature Extraction Algorithms

After the detection of the key points of each PPG pulse, its features can be extracted. Here, we describe the methods utilized to extract features used in the proposed algorithm:

*1) Heart Rate*

According to (1), the heart rate is calculated from the time interval between two consecutive systolic peaks.

*2) mNPV*

To measure mNPV, we use the filtered PPG signal whose dc is not removed. According to (6), mNPV equals the ratio of the peak-to-peak amplitude of the PPG signal divided by its dc value.

*3) Area-Related Features*

The areas confined between every two consecutive key points is considered as a feature. Another utilized feature is the ratio of the area confined between the beginning of the pulse and the inflection point to the area confined between the inflection point and the end of the pulse. The area under the whole pulse is also considered as another feature.

TABLE I
RESULTS BY DIFFERENT MODELS.

| Results | Systolic Blood Pressure (mmHg) | | | | Diastolic Blood Pressure (mmHg) | | | | Mean Blood Pressure (mmHg) | | | |
|---|---|---|---|---|---|---|---|---|---|---|---|---|
| | ME | MAE | STD | CORR | ME | MAE | STD | CORR | ME | MAE | STD | CORR |
| Linear Regression | 0.17 | 16.12 | 10.03 | 0.37 | -0.11 | 7.04 | 5.81 | 0.35 | 0.13 | 8.89 | 6.25 | 0.34 |
| Decision Tree | -0.71 | 13.87 | 15.29 | 0.54 | 0.17 | 6.82 | 8.91 | 0.44 | 0.02 | 8.18 | 9.02 | 0.49 |
| Random Forest | -0.17 | 10.29 | 10.35 | 0.75 | -0.14 | 5.77 | 5.43 | 0.69 | 0.07 | 6.38 | 6.62 | 0.72 |
| AdaBoost | **0.09** | **8.22** | **10.38** | **0.78** | 0.23 | **4.17** | **4.22** | **0.72** | -0.02 | **4.58** | **5.53** | **0.75** |

*4) Amplitude-Related Features*

The peak-to-peak amplitude of each pulse is normalized to one and the resulting amplitudes of diastolic peak, maximum slope point, inflection point and dicrotic notch are chosen as amplitude-related features.

*5) Time-Related Features*

The inverse of the time interval between the systolic peak and diastolic peak is considered as a measure of the stiffness of the large arteries[19]. Other features in this category include the pulse width as a measure of SVR, the inverse of the time intervals between the systolic peak and the inflection point, between the systolic peak and maximum slope point, and also between the systolic peak and dicrotic notch. The crest time is another feature which is calculated as the time interval between the minimum point and the systolic peak.

*6) HRV Properties*

For each individual, the HRV signal is obtained by calculating the time interval between every two consecutive minimums. The mean, STD, low-frequency component (LF) (0.04 – 0.15 Hz), high-frequency component (HF) (0.15 – 0.40 Hz), the LF/HF ratio and the total power of the HRV signal, located one minute before and one minute after each PPG pulse, are the features in this category.

*7) Non-Linear Functions of the Features*

In order to take into account the non-linear relationship between the extracted feature and the BP, a number of non-linear functions of the features are also used as features. The non-linear functions that are used are the logarithm and exponential functions of HR, mNPV and the logarithm of dicrotic notch and inflection point reflection indices. Also, according to the proven relationship between BP and the logarithm of $mNVP * HR$, this logarithm is also considered as a feature.

## IV. RESULTS

### A. Training and Testing the Models

In order to train the BP estimation models, we first normalized all the features to become zero-mean and unit variance. We used Linear Regression, Decision Tree, Random Forest with a size of 100 trees and AdaBoost with the size of 200 decision tree estimators to estimate each of the systolic and diastolic BPs. Also, we used 10-fold cross validation method to divide the data into training and testing sets. It is worth mentioning that, in the UCI dataset, the PPG recordings belonging to each subject are placed consecutively in the dataset but do not have a common identification number. As a result, in order to prevent the overlapping of training and testing subjects, no shuffling was applied and the order of samples in the dataset was retained.

In Table I, Mean Error, MAE, STD and the correlation coefficient between the real and the estimated values are shown. Based on these results, Random Forest and AdaBoost ensemble methods have outperformed simpler methods such as Linear Regression and Decision Tree. Fig. 9 shows the histograms of the estimation errors of the AdaBoost model for the systolic and diastolic BP. As it is seen, the error values are distributed around zero and have a pseudo-symmetric normal distribution. Fig. 10 (a) and Fig. 11 (a) show the scatter plot of the estimated versus real values for systolic and diastolic BP, respectively. As is seen, there is a correlation coefficient of 0.78 for the systolic BP and 0.72 for the diastolic one.

It is important to note that according to Fig. 4, most of the BP values in the UCI dataset are around the normal values. Therefore, in order to better evaluate the performance of the proposed method in abnormal BPs, where the accurate estimation is more critical, we created two subsets of low BP values and high BP values for each of systolic and diastolic BPs. The plots of the estimated versus real values in the low and high values of systolic BP are shown in Fig. 10 (b) and (c) and the ones for diastolic BPs are shown in Fig. 11 (b) and (c). As is seen, correlation coefficients of 0.41 and 0.29 are obtained for low and high systolic BP values, respectively, and correlation coefficients of 0.56 and 0.35 are obtained for low and high diastolic BP values, respectively.

### B. Compatibility with BP Measurement Standards

AAMI-SP10 [46], published by the Association for the Advancements of Medical Instrumentation, defines the requirements that a BP measurement method should meet. According to this protocol with the mercuric sphygmomanometer as a reference, the Mean and the STD of the errors for the measured BP should not be more than 5 mmHg and 8 mmHg, respectively. Moreover, based on this protocol, the number of individuals who undergo BP measurement should be at least 85 to ensure the accuracy of the instrument or the method. Table II compares our results with the requirement for the AAMI standards.

Based on Britain Hypertension Society (BHS) standard [47], if the MAE and STD of more than 60 percent of the test data is less than 5 mmHg and 8 mmHg respectively, then the method will be considered as Grade A. Table III compares our

This article has been accepted for publication in a future issue of this journal, but has not been fully edited. Content may change prior to final publication. Citation information: DOI 10.1109/JSEN.2019.2961411, IEEE Sensors Journal



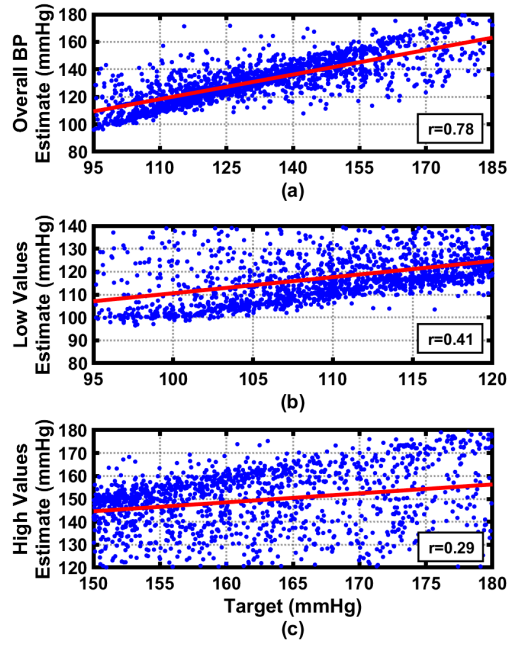


Fig. 10. Regression plot for systolic blood pressure estimation. a) Overall blood pressure regression with r=0.78. b) Low values regression with r=0.41. c) High values regression with r=0.29.

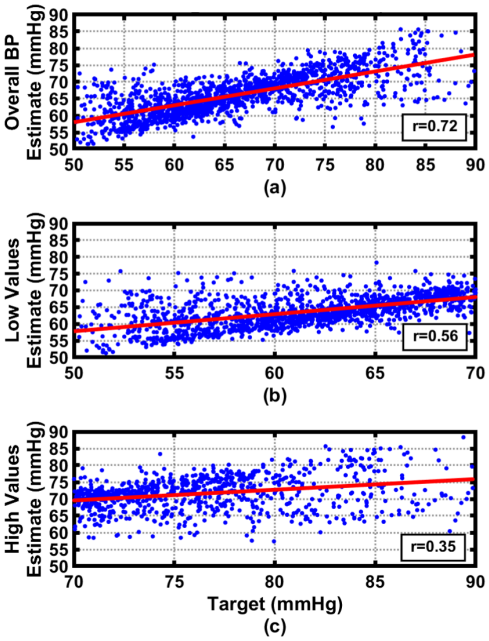


Fig.11. Regression plot for diastolic blood pressure estimation. a) Overall blood pressure regression with r=0.72. b) Low values regression with r=0.56. c) High values regression with r=0.35.

results with the requirement for the BHS standard. Based on this table, we have achieved Grade A for Diastolic, Grade B for Mean and Grade C for Systolic BP.

Another guideline, which is provided jointly by the European Society of Hypertension (ESH) and European Society of Cardiology (ESC) [48], categorizes hypertension into seven classes. We assigned one of the seven different labels to each of the ground truth and estimated BP values

TABLE II

COMPARISON OF OUR RESULTS WITH AAMI STANDARD.

| | | ME (mmHg) | STD (mmHg) | Subjects |
|---|---|---|---|---|
| Results | Diastolic | 0.23 | 4.22 | 942 |
| | Mean BP | -0.02 | 5.53 | 942 |
| | Systolic | 0.09 | 10.38 | 942 |
| AAMI | SBP and DBP | ≤ 5 | ≤ 8 | ≥ 85 |

TABLE III

COMPARISON OF OUR RESULTS WITH BHS STANDARD

| | | Cumulative Error Percentage | | |
|---|---|---|---|---|
| | | ≤ 5mmHg | ≤ 10mmHg | ≤ 15mmHg |
| Results | DBP | 63.2% | 87.9% | 96.3% |
| | MAP | 58.7% | 82.8% | 93.5% |
| | SBP | 44.2% | 70.4% | 89.3% |
| BHS | grade A | 60% | 85% | 95% |
| | grade B | 50% | 75% | 90% |
| | grade C | 40% | 65% | 85% |

resulted from our Adaboost regression method for the purpose of evaluating the ability of the proposed algorithm in the classification of different hypertension levels. The resulting confusion matrix along with the sensitivity, specificity and F-score for each class is shown in Table IV. As is seen, the average sensitivity, specificity and F-score over all classes are 69.3%, 87.7%, and 68.4%, respectively.

### C. *Comparison with Other Works*

Table V compares our results with the previously published methods that use only PPG for BP estimation. The same dataset that we have used, i.e. UCI dataset, is also used in [49]. As is seen in Table V, our proposed method has resulted in smaller estimation errors for systolic and diastolic BPs compared to the method proposed in [49]. We believe that this is due to using additional features, such as mNPV and HRV properties, as well as using more accurate methods for detecting key points in the signals. As mentioned in Sec. II.*C*, there are 12000 signal parts from 1000 persons in the UCI dataset, and as such, many signal parts belong to the same individuals. It seems that in [49], all 12000 signals were shuffled and then partitioned to training and test sets. This means that in [49], some samples of the test subjects were in the training sets, which makes the estimation task significantly easier compared to our case where no sample from the test subjects are in the training set.

In the work presented in [17], the relationships between BP and mNPV and also between BP and HR features are analyzed. The dataset used in [17] consists of the PPG signals and BP values recorded from only 13 individuals. An average correlation coefficient of 0.73 between the estimated and the measured values of BP has been claimed in [17]. To better investigate the effect of the $\ln(HR * mNPV)$ feature on BP

This article has been accepted for publication in a future issue of this journal, but has not been fully edited. Content may change prior to final publication. Citation information: DOI 10.1109/JSEN.2019.2961411, IEEE Sensors Journal



TABLE IV
THE CONFUSION MATRIX OF BP LEVEL CLASSIFICATION

| BP Level Classification Results based on ESH/ESC Guidelines (%) | | Predicted Class: Optimal SBP < 120 and DBP < 80 | Normal 120-129 and/or 80-84 | High Normal 130-139 and/or 85-89 | Grade 1 Hypertension 140-159 and/or 90-99 | Grade 2 Hypertension 160-179 and/or 100-109 | Grade 3 Hypertension ≥ 180 and/or ≥ 110 | Isolated Systolic Hypertension ≥ 140 and < 90 | F-score | Sensitivity | Specificity | Percent of Actual Class Members |
|---|---|---|---|---|---|---|---|---|---|---|---|---|
| Actual Class | Optimal | **79.4** | 16.4 | 2.5 | 0.5 | 0.6 | 0.4 | 0.2 | 76.9 | 79.4 | 80.9 | 35.6 |
| | Normal | 20.1 | **72.2** | 5.4 | 1.0 | 0.2 | 0.7 | 0.4 | 65.1 | 72.2 | 85.3 | 19.3 |
| | High Normal | 9.0 | 10.0 | **74.8** | 4.2 | 1.3 | 0.2 | 0.5 | 72.4 | 74.8 | 91.7 | 16.2 |
| | Grade 1 Hypertension | 13.5 | 5.8 | 10.6 | **65.1** | 1.4 | 2.9 | 0.7 | 71.4 | 65.1 | 94.6 | 18.7 |
| | Grade 2 Hypertension | 11.2 | 8.9 | 8.4 | 17.9 | **45.2** | 7.9 | 0.5 | 54.2 | 45.2 | 98.3 | 5.3 |
| | Grade 3 Hypertension | 19.6 | 12.5 | 14.8 | **21.9** | 15.2 | 14.3 | 1.7 | 12.0 | 14.3 | 98.1 | 1.3 |
| | Isolated Systolic Hypertension | **28.1** | 11.5 | 17.1 | 27.4 | 7.2 | 0.6 | 8.1 | 13.6 | 8.1 | 99.4 | 3.6 |
| **Average** | | | | | | | | | **68.4** | **69.3** | **87.7** | |

TABLE V
COMPARISON WITH OTHER PUBLISHED WORKS

| Work / Publication Year | Subjects (evaluation) | DBP STD (mmHg) | DBP MAE (mmHg) | DBP r | MAP STD (mmHg) | MAP MAE (mmHg) | MAP r | SBP STD (mmHg) | SBP MAE (mmHg) | SBP r |
|---|---|---|---|---|---|---|---|---|---|---|
| **This work** | **942** | **4.22** | **4.17** | **0.72** | **5.53** | **4.58** | **0.75** | **10.38** | **8.22** | **0.78** |
| **Proposed method in [17] on UCI dataset** | 942 | 8.11 | 6.34 | 0.27 | 9.23 | 8.07 | 0.29 | 12.46 | 14.81 | 0.34 |
| [17] / 2018 | 13 | - | - | 0.77 | - | - | 0.74 | - | - | 0.69 |
| [49] / 2017 | 910 | 5.8 | 4.34 | - | - | - | - | 10.9 | 8.54 | - |
| [50] / 2019 | 265 | - | - | - | - | - | - | 9.15 | - | 0.78 |

estimation, we trained a Linear Regression model using only the $\ln(HR * mNPV)$ feature. The results, written in the second row of Table V, show a relatively low correlation coefficient between the estimated and real BP values and also a high MAE in the UCI dataset. Our work shows that by using other PPG features alongside the $\ln(HR * mNPV)$ feature, the correlation coefficient and the accuracy of the model will significantly improve.

### D. Noise Study

PPG signal is usually contaminated by different types of noise such as instrumental and environmental ones. Also, sensor displacements and subject movements can cause base-line wandering. Given that the proposed algorithm in this work is based on extracting different PPG morphological features, different levels of noise and base-line wandering can affect the performance of the algorithm, and as a result, they can decrease BP estimation accuracy. In this section, we investigate the performance of the proposed algorithm in different Signal-to-Noise Ratios (SNRs) and different base-line wandering levels. Accurate extraction of features is directly correlated to the accurate detection of key points such as maximum slope point, systolic peak, dicrotic notch, inflection point, and diastolic peak. As a result, we study the effect of noise on the first two steps of the proposed algorithm, i.e., pre-processing and key-points detection. To that end, we manually added different levels of white Gaussian noise to raw PPG signals and subsequently performed pre-processing and key-points detection. Afterward, we calculated the time displacement between each corresponding key point in the noisy and raw PPG signals as an error. We then calculated the mean absolute and mean STD of these errors and averaged them among all the samples. Also, at each SNR level, MAE of MAP estimation was measured to evaluate the effects of noise on the overall performance of the BP estimation algorithm. Fig. 12 shows a sample PPG signal in different SNRs. Fig. 13 shows the calculated time errors and also BP estimation accuracy at different SNRs. As shown, the errors at SNRs higher than 15dB are tolerable and the proposed algorithm can still estimate the BP with a reasonable accuracy.

Similarly, to study the effect of base-line wandering, we added low frequency sinusoids with different frequencies to raw PPG signals and investigated their effects in the pre-processing step. Results show that our proposed algorithm can reject almost all of the base-line wanders.

## V. DISCUSSION

One of the limitations of the utilized dataset is that the numbers of high and low BP samples in the dataset are considerably smaller than that of normal ones. This led to a fewer number of samples with BP values in these intervals for

This article has been accepted for publication in a future issue of this journal, but has not been fully edited. Content may change prior to final publication. Citation information: DOI 10.1109/JSEN.2019.2961411, IEEE Sensors Journal



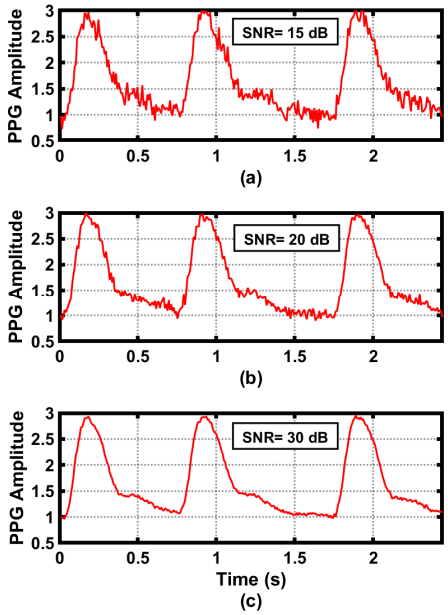


Fig. 12. The effects of noise on PPG signal in different SNRs. a) High level of noise (SNR=15dB), b) average Level of noise (SNR=20dB), and c) low level of noise (SNR=30dB).

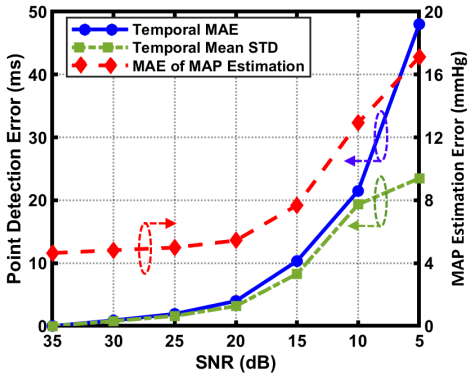


Fig. 13. Mean absolute and mean STD of temporal error in the corresponding detected key points are shown in blue and green, respectively. MAP in each SNR is shown in red.

training the models. Consequently, lower correlation coefficients were obtained compared to samples with BP values in the middle range. This problem is more noticeable when looking at the classification results in Table IV. As is seen, when the percentage of actual class members decreases, the accuracy of the algorithm also decreases.

It is also worth mentioning that the used dataset included signals that were recorded from patients in Intensive Care Units (ICU) and, as a result, the data mainly encompassed those who were in abnormal conditions or had been on medications, which itself, could affect the signals and their relations to BP. In addition, there is no published information regarding the instruments that recorded the signals, and therefore the variations in recording errors could also adversely affect the quality of the results.

The obtained results show that, for estimating the systolic

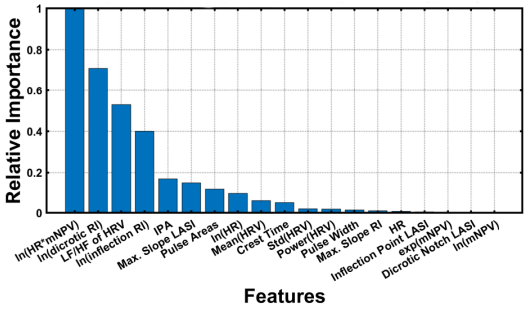


Fig. 14. The relative importance of features in the Mean BP estimation. The values are extracted from the AdaBoost model with Decision Tree Regressor as its estimator and information gain criterion for feature selection.

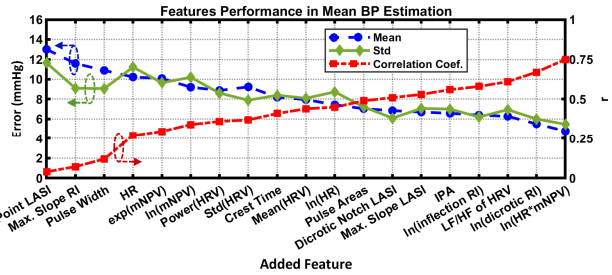


Fig. 15. The trend of mean BP estimation error and corrolation coeeficient versus added features. From left to right, new features are added to the previou ones.

BP, the logarithm of dicrotic notch RI and the logarithm of $HR * mNPV$ are the most important features, and for estimating the diastolic BP, the logarithm of $HR * mNPV$ and the logarithm of inflection point RI are the most important features.

Fig. 14 shows the relative importance of the features for estimating the mean BP. As is seen, in addition to the logarithm of $HR * mNPV$ and the logarithm of dicrotic RI, the LF/HF components of HRV have significant importance in BP estimation.

In Fig. 15, the effects of adding different features on the performance of our BP estimation method is shown. From left to right, in each step, one feature was added to the previous ones and then, an AdaBoost model was trained. Subsequently, MAE, STD and correlation coefficient between the estimated and real mean BP values were calculated and plotted. As is seen, in the last two steps there is an increment of about 0.13 in correlation coefficient, which emphasizes the importance of the logarithm of $HR * mNPV$ and the logarithm of dicrotic RI features in BP estimation. Also, there is a jump in the third step which indicates a strong relationship between the BP and the heart rate.

Among the models, AdaBoost generated the lowest MAE value and the highest correlation coefficient, which demonstrates the better performance of non-linear and ensemble models in estimating BP.

## VI. Conclusion

The ability to estimate the BP of a person from his PPG signal provides three important possibilities: first, estimating the BP of an individual without using a cuff, second,

continuous monitoring of the BP of an individual without periodically inflating a cuff around his arm, and third, estimating the BP of a person using the LED light and the camera of his smartphone.

In this paper, we used the morphological features of the PPG signal to estimate BP. As PPG signals have different shapes in different people, algorithms with low sensitivities to these differences were designed for detecting the key points of the PPG signal. Using 14 features, along with the nonlinear function of a few of them, and also utilizing an ensemble learning method, we have achieved a correlation coefficient of 0.78 for the systolic BP and a correlation coefficient of 0.72 for the diastolic one between the estimated and the real values. Our results fulfill AAMI-SP10 standard requirements for diastolic and mean BPs, and achieve grade A for diastolic, grade B for mean and grade C for systolic BPs based on the BHS standard.

## REFERENCES


[1] M. E. Alnaeb, N. Alobaid, A. M. Seifalian, D. P. Mikhailidis, and G. Hamilton, "Optical techniques in the assessment of peripheral arterial disease," *Curr. Vasc. Pharmacol.*, vol. 5, no. 1, pp. 53–59, 2007.

[2] R. J. Portman and R. J. Yetman, "Clinical uses of ambulatory blood pressure monitoring," *Pediatr. Nephrol.*, vol. 8, no. 3, pp. 367–376, 1994.

[3] J. George and T. MacDonald, "Home blood pressure monitoring," *Eur. Cardiol. Rev.*, vol. 10, no. 2, p. 95, 2015.

[4] T. Arakawa, "Recent research and developing trends of wearable sensors for detecting blood pressure," *Sensors*, vol. 18, no. 9, p. 2772, 2018.

[5] N. Watanabe *et al.*, "Development and validation of a novel cuff-less blood pressure monitoring device," *JACC Basic to Transl. Sci.*, vol. 2, no. 6, pp. 631–642, 2017.

[6] A. J. Coats, "Benefits of ambulatory blood pressure monitoring in the design of antihypertensive drug trials.," *Blood Press. Monit.*, vol. 1, no. 2, pp. 157–160, 1996.

[7] K. Matsumura and T. Yamakoshi, "iPhysioMeter: a new approach for measuring heart rate and normalized pulse volume using only a smartphone," *Behav. Res. Methods*, vol. 45, no. 4, pp. 1272–1278, 2013.

[8] S. Lee and J.-H. Chang, "Deep learning ensemble with asymptotic techniques for oscillometric blood pressure estimation," *Comput. Methods Programs Biomed.*, vol. 151, pp. 1–13, 2017.

[9] Z. Xu, J. Liu, X. Chen, Y. Wang, and Z. Zhao, "Continuous blood pressure estimation based on multiple parameters from eletrocardiogram and photoplethysmogram by Back-propagation neural network," *Comput. Ind.*, vol. 89, pp. 50–59, 2017.

[10] S. Deb, A. Agrawal, and N. Kumar, "Cuffless BP measurement using a correlation study of pulse transient time and heart rate," 2016.

[11] F. W. Xuan, "An exploration on real-time cuffless blood pressure estimation for e-home healthcare." Ph. D. dissertation, University of Macau, 2011.

[12] C. C. Y. Poon and Y. T. Zhang, "Cuff-less and noninvasive measurements of arterial blood pressure by pulse transit time," in *Engineering in Medicine and Biology Society, 2005. IEEE-EMBS 2005. 27th Annual International Conference of the*, 2006, pp. 5877–5880.

[13] B. Gribbin, A. Steptoe, and P. Sleight, "Pulse wave velocity as a measure of blood pressure change," *Psychophysiology*, vol. 13, no. 1, pp. 86–90, 1976.

[14] M. Kachuee, M. M. Kiani, H. Mohammadzade, and M. Shabany, "Cuffless blood pressure estimation algorithms for continuous health-care monitoring," *IEEE Trans. Biomed. Eng.*, vol. 64, no. 4, pp. 859–869, 2017.

[15] A. Esmaili, M. Kachuee, and M. Shabany, "Nonlinear Cuffless Blood Pressure Estimation of Healthy Subjects Using Pulse Transit Time and Arrival Time," *IEEE Trans. Instrum. Meas.*, vol. 66, no. 12, pp. 3299–3308, 2017.

[16] A. M. Johnson, R. Jegan, and X. A. Mary, "Performance measures on blood pressure and heart rate measurement from PPG signal for biomedical applications," in *Innovations in Electrical, Electronics, Instrumentation and Media Technology (ICEEIMT), 2017 International Conference on*, 2017, pp. 311–315.

[17] K. Matsumura, P. Rolfe, S. Toda, and T. Yamakoshi, "Cuffless blood pressure estimation using only a smartphone," *Sci. Rep.*, vol. 8, no. 1, p. 7298, 2018.

[18] K. Matsumura, T. Yamakoshi, H. Noguchi, P. Rolfe, and Y. Matsuoka, "Fish consumption and cardiovascular response during mental stress," *BMC Res. Notes*, vol. 5, no. 1, p. 288, 2012.

[19] S. C. Millasseau, R. P. Kelly, J. M. Ritter, and P. J. Chowienczyk, "Determination of age-related increases in large artery stiffness by digital pulse contour analysis," *Clin. Sci.*, vol. 103, no. 4, pp. 371–377, 2002.

[20] A. A. Awad *et al.*, "The relationship between the photoplethysmographic waveform and systemic vascular resistance," *J. Clin. Monit. Comput.*, vol. 21, no. 6, pp. 365–372, 2007.

[21] A. C. Guyton and J. E. Hall, "Human physiology and mechanisms of disease," 1992.

[22] J. M. Padilla, E. J. Berjano, J. Saiz, L. Facila, P. Diaz, and S. Merce, "Assessment of relationships between blood pressure, pulse wave velocity and digital volume pulse," in *Computers in Cardiology, 2006*, 2006, pp. 893–896.

[23] L. Wang, E. Pickwell-MacPherson, Y. P. Liang, and Y. T. Zhang, "Noninvasive cardiac output estimation using a novel photoplethysmogram index," *Proc. 31st IEEE EMBS*, pp. 1746–1749, 2009.

[24] S. R. Alty, N. Angarita-Jaimes, S. C. Millasseau, and P. J. Chowienczyk, "Predicting arterial stiffness from the digital volume pulse waveform," *IEEE Trans. Biomed. Eng. BME*, vol. 54, no. 12, p. 2268, 2007.

[25] J. Lee *et al.*, "Validation of normalized pulse volume in the outer ear as a simple measure of sympathetic activity using warm and cold pressor tests: towards applications in ambulatory monitoring," *Physiol. Meas.*, vol. 34, no. 3, p. 359, 2013.

[26] K. Matsumura, K. Shimizu, P. Rolfe, M. Kakimoto, and T. Yamakoshi, "Inter-Method Reliability of Pulse Volume Related Measures Derived Using Finger-Photoplethysmography," *J. Psychophysiol.*, 2017.

[27] Y. Sawada, G. Tanaka, and K. Yamakoshi, "Normalized pulse volume (NPV) derived photo-plethysmographically as a more valid measure of the finger vascular tone," *Int. J. Psychophysiol.*, vol. 41, no. 1, pp. 1–10, 2001.

[28] M. E. Gregg, T. A. Matyas, and J. E. James, "A new model of individual differences in hemodynamic profile and blood pressure reactivity," *Psychophysiology*, vol. 39, no. 1, pp. 64–72, 2002.

[29] A. Sherwood, C. A. Dolan, and K. C. Light, "Hemodynamics of blood pressure responses during active and passive coping," *Psychophysiology*, vol. 27, no. 6, pp. 656–668, 1990.

[30] G. Lin *et al.*, "Heart rate variability biofeedback decreases blood pressure in prehypertensive subjects by improving autonomic function and baroreflex," *J. Altern. Complement. Med.*, vol. 18, no. 2, pp. 143–152, 2012.

[31] G.-L. Xie, J. Wang, Y. Zhou, H. Xu, J.-H. Sun, and S.-R. Yang, "Association of high blood pressure with heart rate variability in children," *Iran. J. Pediatr.*, vol. 23, no. 1, p. 37, 2013.

[32] E. R. Carthy *et al.*, "Cardiovascular responsiveness to sympathoexcitatory stress in subjects with and without mild hypertension," *Clin. Physiol. Funct. Imaging*, vol. 35, no. 2, pp. 150–158, 2015.

[33] K. Chaudhary, R. K. Gupta, S. Telles, and A. Balkrishna, "A Correlation between Heart Rate Variability (HRV) and somatization of stress," *Indian J Physiol Pharmacol*, vol. 60, no. 5, 2016.

[34] W.-H. Lin, D. Wu, C. Li, H. Zhang, and Y.-T. Zhang, "Comparison of heart rate variability from PPG with that from ECG," in *The International Conference on Health Informatics*, 2014, pp. 213–215.

[35] V. Jeyhani, S. Mahdiani, M. Peltokangas, and A. Vehkaoja, "Comparison of HRV parameters derived from photoplethysmography and electrocardiography signals," in *Engineering in Medicine and Biology Society (EMBC), 2015 37th Annual International Conference of the IEEE*, 2015, pp. 5952–5955.

[36] A. L. Goldberger *et al.*, "PhysioBank, PhysioToolkit, and PhysioNet: components of a new research resource for complex physiologic signals," *Circulation*, vol. 101, no. 23, pp. e215--e220, 2000.

[37] A. Choi and H. Shin, "Photoplethysmography sampling frequency: pilot assessment of how low can we go to analyze pulse rate variability with reliability?," *Physiol. Meas.*, vol. 38, no. 3, p. 586, 2017.

[38] S. Mahdiani, V. Jeyhani, M. Peltokangas, and A. Vehkaoja, "Is 50 Hz high enough ECG sampling frequency for accurate HRV analysis?," in *2015 37th Annual International Conference of the IEEE Engineering in Medicine and Biology Society (EMBC)*, 2015, pp. 5948–5951.

[39] Y. Nishikawa, S. Izumi, Y. Yano, H. Kawaguchi, and M. Yoshimoto, "Sampling Rate Reduction for Wearable Heart Rate Variability Monitoring," in *2018 IEEE International Symposium on Circuits and Systems (ISCAS)*, 2018, pp. 1–5.

[40] A. L. Jacobson, "Auto-threshold peak detection in physiological signals," in *Engineering in Medicine and Biology Society, 2001. Proceedings of the 23rd Annual International Conference of the IEEE*, 2001, vol. 3, pp.

2194–2195.
[41] H. Rabbani, M. P. Mahjoob, E. Farahabadi, and A. Farahabadi, "R peak detection in electrocardiogram signal based on an optimal combination of wavelet transform, hilbert transform, and adaptive thresholding," *J. Med. Signals Sens.*, vol. 1, no. 2, p. 91, 2011.
[42] Q. Xue, Y. H. Hu, and W. J. Tompkins, "Neural-network-based adaptive matched filtering for QRS detection," *IEEE Trans. Biomed. Eng.*, vol. 39, no. 4, pp. 317–329, 1992.
[43] A. T. Tzallas, V. P. Oikonomou, and D. I. Fotiadis, "Epileptic spike detection using a Kalman filter based approach," in *Engineering in Medicine and Biology Society, 2006. EMBS'06. 28th Annual International Conference of the IEEE*, 2006, pp. 501–504.
[44] F. Scholkmann, J. Boss, and M. Wolf, "An efficient algorithm for automatic peak detection in noisy periodic and quasi-periodic signals," *Algorithms*, vol. 5, no. 4, pp. 588–603, 2012.
[45] M. Elgendi, "On the analysis of fingertip photoplethysmogram signals," *Curr. Cardiol. Rev.*, vol. 8, no. 1, pp. 14–25, 2012.
[46] A. for the Advancement of Medical Instrumentation and others, "American national standards for electronic or automated sphygmomanometers," *ANSI/AAMI SP 10-1987*, 1987.
[47] E. O'brien *et al.*, "The British Hypertension Society protocol for the evaluation of automated and semi-automated blood pressure measuring devices with special reference to ambulatory systems.," *J. Hypertens.*, vol. 8, no. 7, pp. 607–619, 1990.
[48] G. Mancia *et al.*, "2013 ESH/ESC guidelines for the management of arterial hypertension: the Task Force for the Management of Arterial Hypertension of the European Society of Hypertension (ESH) and of the European Society of Cardiology (ESC)," *Blood Press.*, vol. 22, no. 4, pp. 193–278, 2013.
[49] M. Liu, L.-M. Po, and H. Fu, "Cuffless Blood Pressure Estimation Based on Photoplethysmography Signal and Its Second Derivative," *Int. J. Comput. Theory Eng.*, vol. 9, no. 3, p. 202, 2017.
[50] D. Fujita, A. Suzuki, and K. Ryu, "PPG-Based Systolic Blood Pressure Estimation Method Using PLS and Level-Crossing Feature," *Appl. Sci.*, vol. 9, no. 2, p. 304, 2019.

**Navid Hasanzadeh** received the B.Sc. degree (with honors) in biomedical engineering from Amirkabir University of Technology (Tehran Polytechnic), Tehran, Iran, in 2018. He also received a minor degree in electrical engineering, with a focus on machine learning from the same university, in 2019.
His research interests include machine learning, deep learning, signal processing, and their applications in healthcare.

**Mohammad Mahdi Ahmadi** (S'05–M'07–SM'19) received the B.Sc. degree in biomedical engineering (Highest Honors) from Shahid Beheshti University, Tehran, Iran, in 2000, the M.Sc. degree in electronic engineering from Sharif University of Technology, Tehran, Iran, in 2002, and the Ph.D. degree in electrical engineering from the University of Calgary,Calgary, AB, Canada, in 2007.
His Ph.D. research was on developing a wireless implantable microsystem for continuous blood glucose monitoring. From 2007 to 2010, he was with Sound Design Technologies Ltd., Burlington, ON, Canada (acquired by ON semiconductor) where he designed ultra low-power and low-voltage analog integrated circuits for hearing aids. From 2010 to 2014, he was with Synopsys Inc., Toronto, Canada, where he designed high-speed circuits for multi-standard multi-Gb/s wireline applications. In the summers of 2015 and 2017, he was with Rambus Inc., Sunnyvale, CA, USA, and in the summers of 2018 and 2019, he was with Analog Bits Inc., Sunnyvale, CA, USA, designing high-speed wireline circuits. Since 2014, he has been an Assistant Professor with the Department of Biomedical Engineering, Amirkabir University of Technology, Tehran, Iran. His research interests include integrated circuit and system design for biomedical and communication applications.
Dr. Ahmadi was the recipient of awards at the 44th ISSCC/DAC and the third Analog Devices student circuit design contests. He was part of a team which received the 2010 EDN Innovation award for developing the world's first full system-on-chip for hearing aids.

**Hoda Mohammadzade** received her BSc degree from Amirkabir University of Technology (with honors), Iran, in 2004, the MSc degree from the University of Calgary, Canada, in 2007, and the PhD degree from the University of Toronto, Canada, in 2012, all in electrical engineering.
From 2014, she has been an assistant professor with the department of electrical engineering, Sharif University of Technology, Tehran, Iran.
Her research interests include machine learning, signal and image processing, computer vision, biometric systems, and bioinformatics.